IMPROVED PREDICTIONS OF SOLAR AND GEOMAGNETIC ACTIVITY WITH APPLICATION TO ESA/LEO SATELLITE OPERATIONS

Alan W P Thomson, Jess A King, Ellen Clarke and Toby D G Clark

British Geological Survey, West Mains Road, Edinburgh EH9 3LA, UK,
Email: a.thomson@bgs.ac.uk, t.clark@bgs.ac.uk, e.clarke@bgs.ac.uk

ABSTRACT

The European Space Operations Centre (ESOC) plans a third low Earth orbit observation satellite, ENVISAT, following on from ERS-1 and ERS-2. ESOC requires control of the satellite ground track to ±1 km, placing a strong constraint on the accuracy of thermospheric density modeling and forecasts of the solar and geomagnetic indices that parameterize density models. This paper addresses the accuracy of an index forecast model developed by the British Geological Survey (BGS) for ESOC and used during the ERS satellite missions. Forecast accuracy is shown to have been better than expected although an improved model for the *Ap* geomagnetic index is provided. We also examine the time series of drag coefficients, *Cd*, for the ERS satellites, in relation to readily available solar and geomagnetic data. Simple regression models are shown to reduce the standard deviation in *Cd* about the mean by about one fifth, suggesting scope for improvements in density modeling.

1. INTRODUCTION

ESOC currently uses the model *MSIS* for atmospheric density estimates when calculating frictional drag on low Earth orbit satellites such as ERS-1, ERS-2 and, in the future, ENVISAT. *MSIS* is parameterised by the geomagnetic activity index *Ap*, the solar radio flux at 10.7 cm wavelength, $F_{10.7}$, as well as the 81-day smoothed $F_{10.7}$ [1]. Accurate future density estimates for satellite orbit control and manoeuver planning, within the precision afforded by the MSIS algorithm, clearly depend on a good prediction of future values of *Ap* and $F_{10.7}$. In a previous study for ESOC [2] BGS constructed a software package for the forecasting of these indices up to 27 days ahead. This software, PDFLAP (understood as '*P*re*d*iction of *Fl*ux and *Ap*'), has now been in operation since 1992.

A typical PDFLAP forecast of $F_{10.7}$ is shown in Fig. 1. Approximate 50% and 95% confidence limits are provided with the forecast. The PDFLAP algorithm is linear autoregression, where coefficients are recalculated daily to reflect changing solar and geomagnetic conditions. The $F_{10.7}$ filter length is 60 days, the *Ap* filter length is 30 days, both deduced by experimentation. Filter coefficients are derived from the last 24 months of data ($F_{10.7}$) or 6 months of data (*Ap*). In [2] we more fully describe the process of model selection, development and testing. Below we investigate the observed level of accuracy since 1992 and report on an improved prediction algorithm for *Ap*.

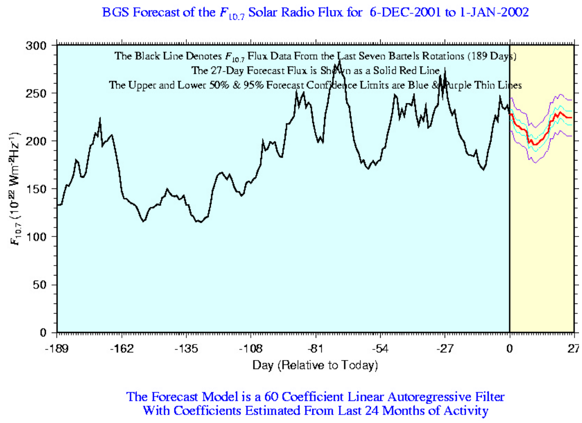

Fig. 1. A typical 27-day prediction of $F_{10.7}$.

We have also investigated those solar and geomagnetic data, beyond *Ap* and $F_{10.7}$, which are now available at least on a next day basis and have attempted to determine whether these data are potentially useful for more accurate forecasts of variations in atmospheric density. Of particular interest are geomagnetic data that describe Joule heating effects from energised current systems at high and polar latitudes during magnetic storms and a new, supposedly more accurate, proxy index for solar ultraviolet emission (and hence ionisation of the upper atmosphere), the $E_{10.7}$ index [3]. We have examined the time series of drag coefficients, *Cd*, for the ERS satellites and investigated whether the observed variability in *Cd* can be related to solar and geomagnetic data. In particular, we investigate whether we can build an effective 'correction' factor for the ERS-2 orbit. Such a correction term may be useful for ENVISAT as it follows a similar orbit.

2. PDFLAP: AN OPERATIONAL SYSTEM FOR SOLAR AND GEOMAGNETIC ACTIVITY PREDICTION

PDFLAP has been in use since 1992 and retrospective tests on past solar cycle data quantified its expected level of accuracy [2]. However we now have accumulated an independent (forecast) data set that covers a substantial fraction of the current and last solar cycles. We have also taken the opportunity to compare the results with some simpler benchmark ‘forecasts’ to provide a context for evaluating the software. Our assessment was based on the following statistical tests:

1. *Forecast - Observed* root-mean-square (*RMS*) error as a function of year and of forward lag. Lags of one day through 27 days are used, as these are the output lags (days) of the software.
2. The percentage of all days where the forecast is within a given tolerance ($\pm N$ units) of the observed value, again as a function of year and lag. We have examined tolerances of ± 5, ± 10, ± 20 units.
3. The computed ‘skill score’ of PDFLAP against other benchmark techniques versus year and lag.

The skill score $SS_{\mathrm{BENCHMARK}}$ (see the list of verification definitions at the Space Environment Center (SEC) site http://www.sec.noaa.gov/forecast_verification/) against a benchmark technique is defined as

$$SS_{\mathrm{BENCHMARK}} = 1 - MSE_{\mathrm{PDFLAP}}/MSE_{\mathrm{BENCHMARK}} \qquad (1)$$

where *MSE* is mean-square-error over all forecasts. A skill score of one implies a perfect PDFLAP forecast, regardless of benchmark. A *SS* of zero implies no difference between the two methods and less than zero implies that the other method has more ‘skill’.

The benchmark techniques examined were

1. Persistence: the forecast for each of 1-27 days ahead is equal to today's observed value. Persistence is known to be strong for geomagnetic indices at one and two days ahead.
2. Recurrence: the forecast for each day up to 27 days ahead is exactly equal to the value observed 27 days before that date. This is based on the tendency towards recurrence in geomagnetic data and is related to the rotation rate of the Sun with respect to the Earth.
3. Climatology: the forecast for 1-27 days ahead is equal to the mean of the observed values of the 27 days up to today. This approach emphasises a current ‘smoothed’ level of activity appropriate to long-term variations that are seen to depend on the smoothed sunspot cycle [4]. Note that this definition of ‘climatology’ differs from other interpretations that tend to emphasise average behaviour over a much longer time span.
4. For *Ap*, we considered a back-propagation neural network model for one to three days ahead [5].

The results comprised data on (and depending on year, solar phase, day-lag, etc)

1. Absolute accuracy.
2. Accuracy relative to that expected [2].
3. Relative accuracy with respect to the benchmarks.
4. Skill scores.

In Figs. 2 to 5 we show the major and most relevant findings of the analysis. Full details are in [6]. We note here that neither persistence nor recurrence showed any merit and are not discussed further.

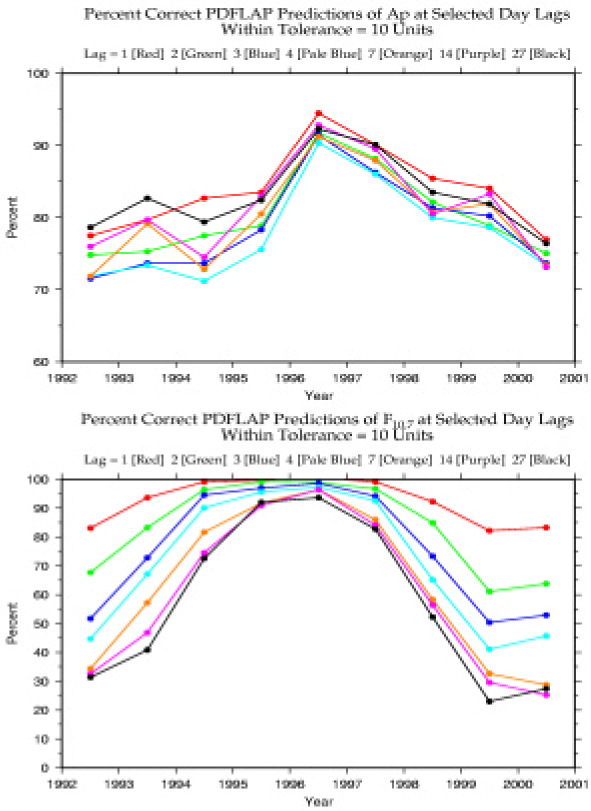

Fig. 2. Accuracy of *Ap* and $F_{10.7}$ predictions within a tolerance of 10 units since 1992. This tolerance level is regarded as ‘desirable’ in mission planning.

No forecast technique for $F_{10.7}$ seems to be clearly preferable to PDFLAP. Indeed, although we have not demonstrated it here, even neural network models of $F_{10.7}$ do not show significant improvement over PDFLAP (based on informal tests of $F_{10.7}$ carried out during the *Ap* study reported in [5]). During the quietest solar conditions $F_{10.7}$ climatology becomes a comparable approach. However it is not obviously superior and we do not judge it good enough to merit a modification of the PDFLAP algorithm. We investigated in [7] a regression model for $F_{10.7}$ based on SEC reports of solar active regions and demonstrated that it provided a marginal improvement over PDFLAP (a few percent at a tolerance of ± 10 units), from about six up to twelve days ahead. However we do not currently believe that this adaptation is yet warranted for day-to-day operations.

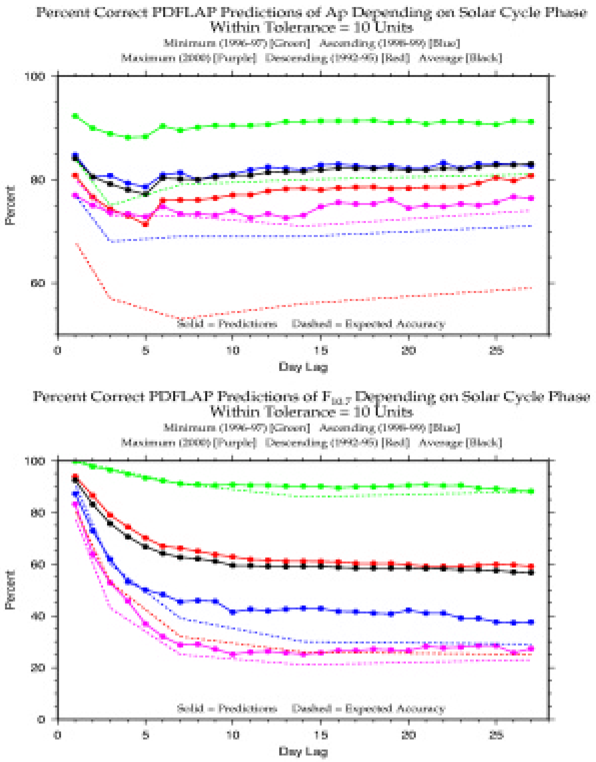

Fig. 3. Accuracy of *Ap* and $F_{10.7}$ predictions as a function of forward forecasting lag compared with expected accuracy based on last two solar cycles [2]. Colour coding denotes solar cycle phase.

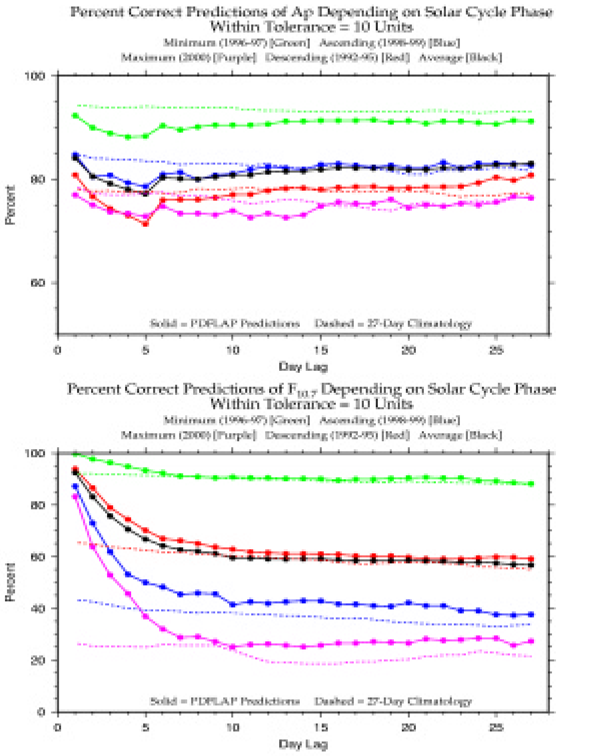

Fig. 4. Accuracy of *Ap* and $F_{10.7}$ predictions as a function of forward forecasting lag compared with 27-day climatology since 1992. Colour coding denotes solar cycle phase.

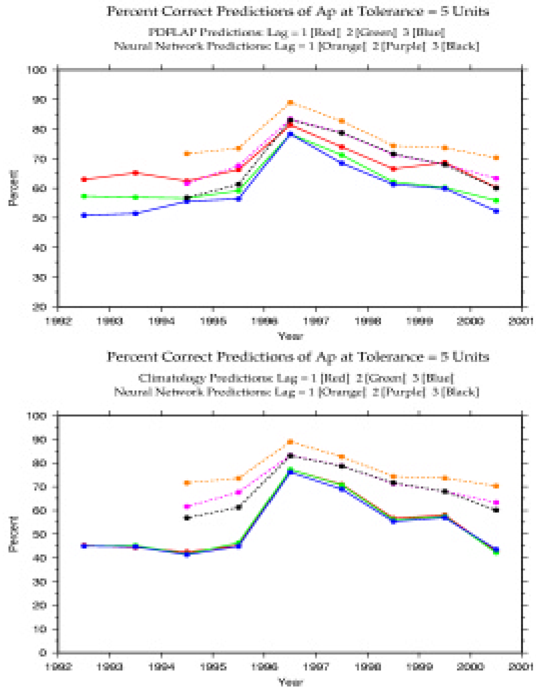

Fig. 5. Accuracy of *Ap* predictions as a function of forward forecasting lag compared with a neural network prediction (since 1994) [5]. Colour coding denotes forward lag and method.

Forecasts of *Ap* have also been more accurate than expected. However, unlike $F_{10.7}$, there are other techniques that have been shown to be at least as useful as the current PDFLAP algorithm, in some solar cycle phases or within some particular tolerances. These are climatology and neural network (i.e. non-linear) models. It should be noted that neural network forecasts of magnetic storms, though better than PDFLAP, may not be as accurate as human forecasts, for example, those which are part of the daily SEC reports.

3. IMPROVED FORECASTS OF *Ap*

Through close examination of results such as in Figs. 2 to 5 we have found that there is room for improvement in geomagnetic activity prediction, principally by taking advantage of non-linear methods such as are provided by neural networks. Physically this may at least partly reflect the non-linearity of processes operating in the magnetosphere. At the same time simple index climatology (as defined above) has also been found to be useful for some forecast lags.

The accuracy of an improved, 'hybrid', *Ap* prediction scheme is presented in Fig. 6. In this algorithm, days 1-3 are forecast by the back-propagation neural net, days 4-6 by climatology, days 7-15 by the existing PDFLAP algorithm and days 16-27 according to the minimum of

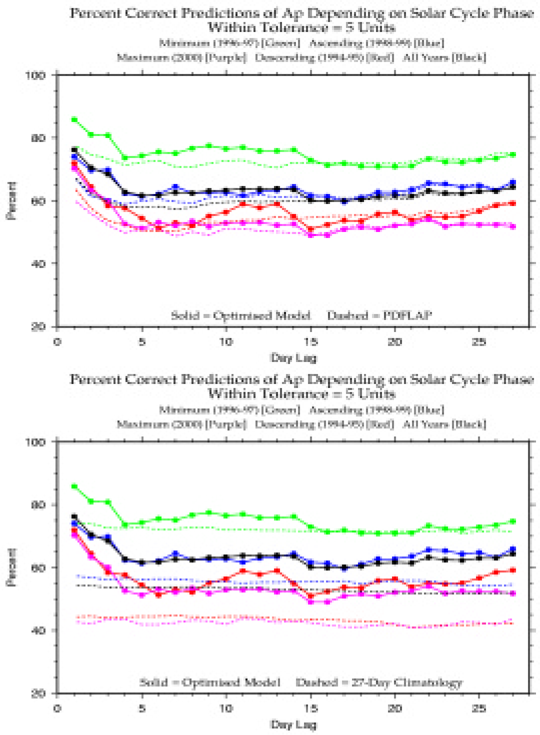

Fig. 6. Prediction accuracy for the new geomagnetic prediction technique compared with the existing PDFLAP and climatology.

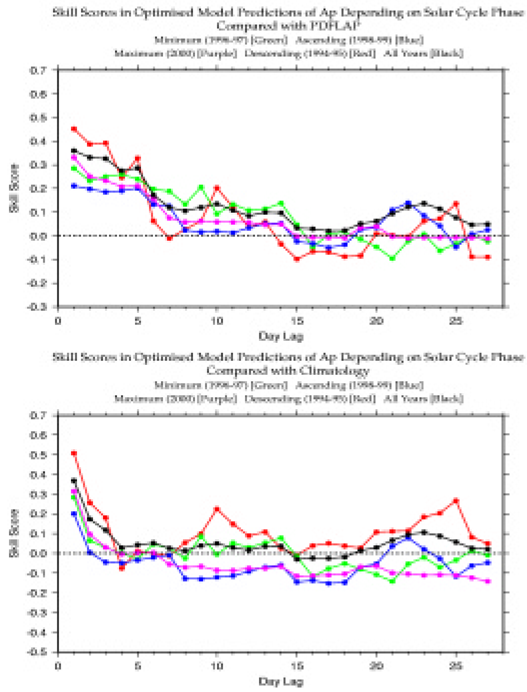

Fig. 7. Skill scores for the new geomagnetic prediction technique compared with the existing PDFLAP and climatology.

climatology and PDFLAP predictions (deduced again by experimentation). Clearly there is little physical justification for the algorithm: it simply performs best on a data set covering the last 8 years and also suggests that regular future checks of accuracy will be needed. In terms of skill scores the improved *Ap* algorithm performs best at the shorter time lags, as shown in Fig. 7. The benchmarks shown in Fig. 7 are the existing PDFLAP algorithm (upper plot) and simple climatology (lower plot). Although there is clearly a dependence on the phase of the solar cycle, on average the new algorithm can be seen to have added value to the existing model.

4. THERMOSPHERIC DRAG AND SOLAR AND GEOMAGNETIC ACTIVITY INDICES

Models such as *MSIS* that use global daily activity parameters such as *Ap* may not capture brief localised heating effects at high latitudes during storms and sub-storms. Similarly, the true EUV ionisation of the atmosphere may not be well represented by the parameter $F_{10.7}$ (known to be more variable than solar EUV [3]). These effects may be better parameterised by solar and geomagnetic indices that are better matched physically to individual processes. In particular the recently introduced $E_{10.7}$ solar EUV index may prove useful [3].

Deficiencies in density models using these data may be revealed in a variation about a constant value of the drag coefficient, *Cd*, for LEO satellites. The drag coefficient *Cd* and modelled atmospheric density, $?_{\mathrm{MODEL}}$, are related in terms of drag force F_D, satellite mass, *m*, acceleration, a_D, cross-sectional area, *A*, and velocity, *V*, as

$$F_D = m \cdot a_D = -½ \cdot Cd \cdot A \cdot ?_{\mathrm{MODEL}} \cdot V^2 \qquad (2)$$

In effect *Cd* represents a scaling factor that represents our ignorance of the true atmospheric density at the satellite location: *Cd* varies with time and position according to the error in the modelled density.

There are two procedures employed by ESOC for computing the orbits of ERS-1 and ERS-2: the *operational* orbit determination and the *precise* orbit determination. The drag coefficients used in this study for both ERS-1 and ERS-2 are derived from the precise orbit determination. The precise orbit makes use of tracking data from Kiruna and other stations in the computation of orbital parameters. The precise orbit is computed using five-day arcs, overlapping by two days. Values are computed for 00:00UT and 12:00UT for each day in the five-day arc. Daily averages are used here.

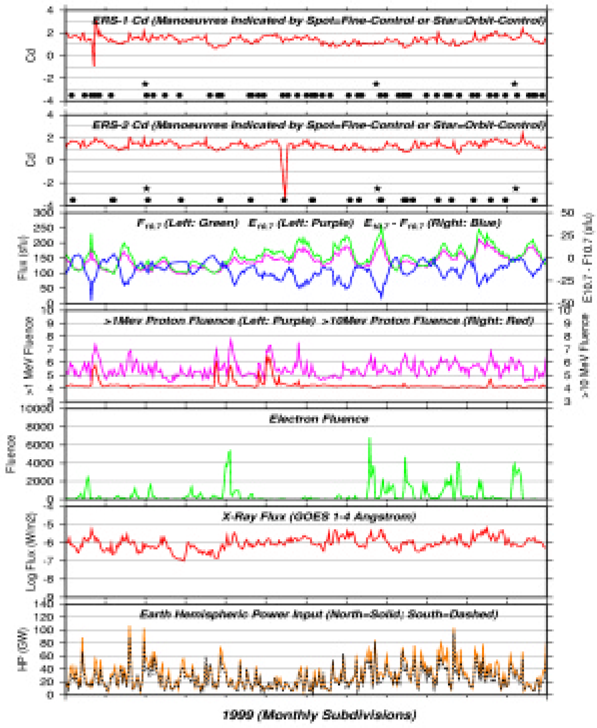

Fig. 8. Stackplot of daily-averaged ERS-1 and ERS-2 drag coefficients compared with various daily solar activity and Earth hemispheric power input data for 1999.

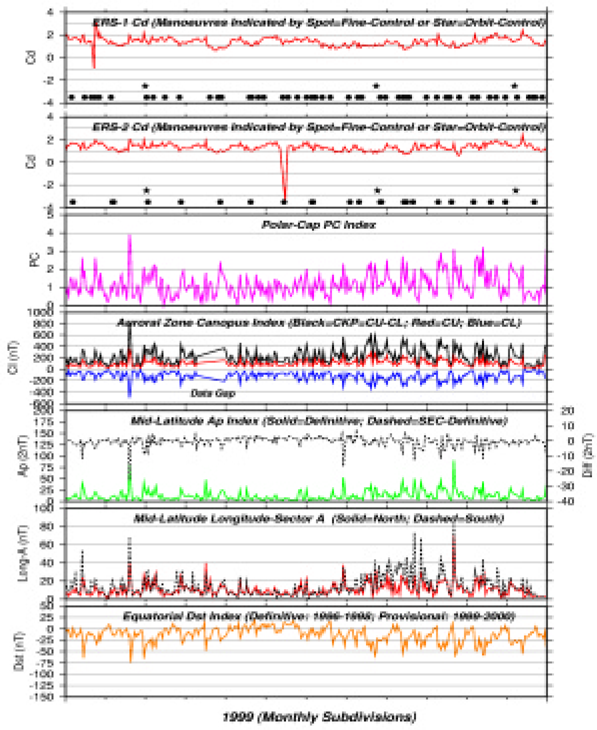

Fig. 9. Stackplot of daily-averaged ERS-1 and ERS-2 drag coefficients compared with various daily geomagnetic activity data for 1999.

In Figs. 8 and 9 we show daily ERS-1 and ERS-2 *Cd* data, in comparison with (daily average) solar and geomagnetic data for 1999. Other years have also been examined (1996-2000) but are not reproduced here.

A strong correlation amongst the geomagnetic data is evident (e.g. ‘peaks’ in *Ap* mirrored by ‘peaks’ in other data). This indicates that the daily geomagnetic data are not independent. With data on a sub-daily time resolution this may not have been true. However, it is seen that at least some of the smaller fluctuations in *Cd* are related to the larger solar and geomagnetic variations. This is the case for both ERS-1 and ERS-2, for which the variations in *Cd* are very similar, indicating that both satellites are subject to similar atmospheric perturbation forces. It is also notable in Fig. 8 that the difference between daily $E_{10.7}$ and $F_{10.7}$ grows in amplitude from solar minimum through solar maximum, sometimes displaying a roughly 27-day periodicity. We note that only those *Cd* between about +0.5 and +3.0 are likely to be related to solar and geomagnetic influences. Other values, particularly negative values, are likely to be related to manoeuvres (from conversation with ESOC), other controller initiated changes, or instrumental effects, drifts, offsets or re-calibrations. For the purposes of further study we therefore ‘prune’ these outliers from the data set.

A linear regression study following on from Figs. 8 and 9 suggests that *Ap*, *PCN* (northern polar cap index), *HPN* (northern hemispheric power index), *Dst* (low-latitude ring current index) and *CKP* (Canopus magnetometer array auroral index) are likely to be useful explanatory geomagnetic variables. Longitude-sector A_i data in the same sector as the ERS-2 satellite are at best of marginal relevance. We also find that differences in the solar data, i.e. $E_{10.7}$ - $F_{10.7}$ and their smoothed values, show most clearly in longer period variations in *Cd*. Note we have only *PC(North)* available for this study, and therefore concentrate on *HPN* rather than *HPS*. Slight differences observed between, for example, *HPN* and *HPS* are worthy of further study. Particle precipitation data are found to be most useful when used in combination with other variables and, in general, systematic experimentation using these and other data has been necessary to find potential ‘best’ regression combinations. In this way we have also found that lagging some variables by one day improves the correlation (reason unclear). However it is interesting to note that the most useful geomagnetic indices reflect geomagnetic activity in particular latitude zones, especially at high and low latitudes, where activity is not characterized by *Ap*. Also, particle precipitation into the magnetosphere at very high latitudes may be a relevant indicator of heating.

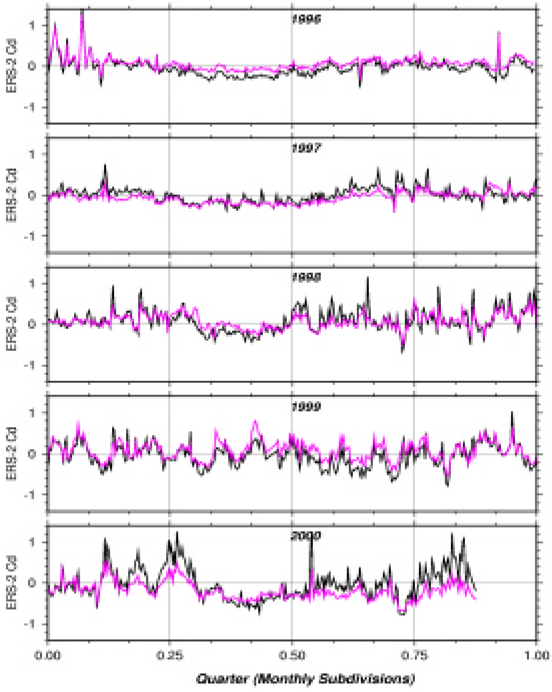

Fig. 10. The variance in *Cd* for ERS-2 (black) is reduced by the optimum regression on solar and geomagnetic data (purple). The correction factor is multiplicative. Mean *Cd* is subtracted.

In Fig. 10 we compare the ERS-2 *Cd* (black line) with the improved *Cd* (coloured line), where the best regression relationship is multiplicatively taken into account. (Note: a perfect correlation would reduce the *Cd* variability to zero.) Although there are a number of regression relationships that all reduce the variance in *Cd*, in Fig. 10 we use the correlation that proves optimum for this data set. This regresses *Cd* on *Ap*, *PC(North)*, proton fluence and $E_{10.7}$ - $F_{10.7}$. Finally, in Table 1 we quantify the observed reduction in *Cd* variance. These figures seem to mirror similar results reported by the US Air Force [8], using a 'calibration satellite' approach.

Table 1 A comparison of original and corrected mean and standard deviation (SD) in *Cd*.

	Original Data	***After Correction by ERS-2 Cd Model***	***Reduction in % Ratio of SD/Mean***
ERS-1	**1.370±0.313 (SD=22.8% of Mean)**	**1.397±0.252 (SD=18.0% of Mean)**	**4.8%**
ERS-2	**1.365±0.272 (SD=19.9%)**	**1.365±0.210 (SD=15.4%)**	**4.5%**

5. CONCLUSIONS

An analysis of the accuracy of the PDFLAP forecast code has been made, covering the period January 1992 to December 2000, or nearly a full solar cycle. The observed accuracy of the forecast models of the $F_{10.7}$ solar radio flux and the *Ap* geomagnetic activity index is shown to have been better than anticipated [2]. Even so, an improved prediction model for *Ap* has been derived and evaluated. No improvement has been found or is suggested from the present work for $F_{10.7}$. We have examined the time series of drag coefficients for ERS-1 and ERS-2 and produced regression relationships with solar and geomagnetic indices. The best model reduces the standard deviation about each mean coefficient from about 23% and 20% of the mean, respectively for ERS-1 and ERS-2, to about 18% and 15%, or approximately by about one fifth. These regression models may prove useful for improved control for ENVISAT given the similarity of its orbit to that of ERS-2. We have also noted the importance of the difference between the $E_{10.7}$ index and $F_{10.7}$ index in those 27-day and longer period variations seen in *Cd* and the need for further study of these terms. Finally we note that further progress on drag modelling may well require sub-daily data, rather than daily averages.

6. ACKNOWLEDGEMENTS

Roberta Mugellesi-Dow, Dirk Kuijper, Rene Zandbergen, and Heiner Klinkrad of ESOC are thanked for useful discussions on the results here and for providing the drag coefficient data. This paper is published by permission of the Director, BGS (NERC).

7. REFERENCES

1. HEDIN, A E. MSIS-86 Thermospheric Model. *J. Geophys. Res.*, **92**, 4649-4662, 1987.

2. THOMSON, A W P., CLARK, T D G., and KERRIDGE, D J. Computer Algorithms & FORTRAN Programs for Forecasting Solar and Geomagnetic Activity in the Short-term. *BGS Technical Report*, WM/92/19C, 1992.

3. TOBISKA, W K., and EPARVIER F. EUV97: Improvements to EUV Irradiance Modeling in the Soft X-Rays and FUV. *Sol. Phys.*, 177, 147-159, 1998.

4. FEYNMAN, J., and GU X Y. Prediction of Geomagnetic Activity on Time Scales of One to Ten Years. *Rev. Geophys.*, 24, 650, 1986.

5. THOMSON, A W P. Non-linear Predictions of *Ap* by Activity Class Numerical Value. *Pure App. Geophys.*, **146** (1), 163-193, 1996.

6. THOMSON, A W P., KING, J A., CLARKE, E. and CLARK, T D G. Improved Predictions of Solar and Geomagnetic Influence on the Near Earth Environment. *BGS Technical Report*, CR/01/61, 2001.

7. THOMSON, A W P., CLARKE, E., and CLARK, T D G. 1995. Study on Forecasting of Solar and Geomagnetic Activity, Phase 2 *BGS Technical Report*, WM/95/16C, 1995.

8. STORZ, M F. High Accuracy Satellite Drag Model. *Space Weather Week 2001*, Space Environment Center, Boulder Co., 2001.